Soft Matter

PAPER

View Article Online
View Journal | View Issue

Cite this: *Soft Matter*, 2020, **16**, 709

Strong adhesion of poly(vinyl alcohol)–glycerol hydrogels onto metal substrates for marine antifouling applications†

Heng-Wei Zhu,[a] Jia-Nan Zhang,[a] Pei Su,[b] Tianqi Liu,[a] Changcheng He,*[a] Danqing Feng*[b] and Huiliang Wang [a]

Hydrogels can be used as an alternative coating material for ships against marine biofouling. However, the adhesion of wet and soft hydrogels onto solid metals remains a challenging problem. Here we report the adhesion of a typical hydrogel material, poly(vinyl alcohol) (PVA)–glycerol hydrogel, onto stainless steel substrates and the antifouling potency of the adhered PVA–glycerol hydrogels. Poly(allylamine hydrochloride) (PAH) hydrogel and ethyl α-cyanoacrylate (ECA) are used as the binders, and they are found to be able to firmly bond the PVA–glycerol hydrogels onto the stainless steel substrates. The PAH hydrogel does not affect the mechanical properties of the PVA–glycerol hydrogel during use, but it tends to lose the adhesive ability in a dehydrating environment. In contrast, the ECA adhesive can maintain strong bonding between PVA–glycerol hydrogels and substrates upon several water losing/water absorbing cycles, despite some negative effects on the strength of the PVA–glycerol hydrogel. Biological experiments show that the PVA–glycerol hydrogel has a strong settlement-inhibiting effect on the barnacle *Balanus albicostatus*, suggesting that combining the PVA–glycerol hydrogel with ECA adhesive may have promising applications in marine antifouling.

Received 12th July 2019,
Accepted 20th November 2019

DOI: 10.1039/c9sm01413f

rsc.li/soft-matter-journal

1 Introduction

Marine biofouling, the accumulation of marine fouling organisms on submerged surfaces,[1] has been a serious problem for the development of marine economy, since these attached organisms can slow down the vessels and cause extra fuel consumption up to 40%, leading to billions of dollars in waste.[2,3] The fouling organisms can also corrode the surface they are in contact with, resulting in a shortened life of the hulls.[4,5] This problem used to be solved by tin-containing self-polishing coatings since organotin compounds can kill marine organisms efficiently. But the global prohibition of coating with tributyltin (TBT) in 2008, due to its negative effects on marine environments, raised this issue again.[6] Though copper/zinc[7,8] and organic biocides[9–11] are used as substitutes, copper related coatings are also toxic and the toxicity of organic biocides towards marine environments is still under investigation.[12–17] Therefore, environment friendly coatings are urgently needed in the current market. Compared with killing the biofouling organism, preventing or reducing settlement of the fouler on submerged surfaces is more favorable for environment protection.[15] Thus, more researchers are willing to focus on green coatings like fouling release, fouling resistant and non-leaching biocide coatings.[1,18,19] Several green coatings such as PEG-based coatings,[20–22] and PDMS-based coatings[23–25] have been reported in recent years.

Among the diverse coating materials, hydrogels, which are soft and wet materials with 3D networks, are considered to be promising candidates with high antifouling performance against marine organisms. The super hydrophilic characteristic of hydrogel materials makes them absorb a large amount of water into the 3D networks and form a highly hydrated layer on their surface which can prevent the adhesion of proteins or microorganisms. Besides, the swollen hydrogels possess a soft and highly elastic nature while most marine organisms prefer to attach to hard surfaces. Murosaki *et al.*[26,27] investigated the antifouling behaviors of a series of synthetic hydrogels against barnacles both in the laboratory and in a long-term marine environment experiment, and the results actually evidenced the efficient antifouling performance of the hydrogels. However, there is an emerging issue for practical applications regarding how to coat hydrogels onto the required substrates with steady adhesion. Xie *et al.*[28] and Hong *et al.*[29] reported a polymeric coating made of cross-linked poly(methyl methyacrylate-*co*-tributylsilyl

[a] *Beijing Key Laboratory of Energy Conversion and Storage Materials, College of Chemistry, Beijing Normal University, Beijing 100875, P. R. China. E-mail: herbert@bnu.edu.cn*
[b] *State-Province Joint Engineering Laboratory of Marine Bioproducts and Technology, College of Ocean & Earth Sciences, Xiamen University, Xiamen, 361102, P. R. China. E-mail: dqfeng@xmu.edu.cn*

† Electronic supplementary information (ESI) available. See DOI: 10.1039/c9sm01413f

methacrylate-*co*-acrylic acid) terpolymer chains that can be easily applied on a surface by conventional brushing or spraying methods. The surface layer of this coating can gradually hydrolyze and form highly swollen hydrogels once it has made contact with seawater, endowing it with anti-biofouling ability. However, the formed hydrogel layer was unstable and suffered from a continuous generation and peeling process, which caused severe consumption of the coatings during long-term usage. This suggests that the strong mechanical and physicochemical properties of hydrogels, as well as the versatile methods used to apply the hydrogels onto the substrate surface, are both important for practical applications. Unfortunately, there are very limited studies devoted to the advancement of marine antifouling applications of hydrogels, and no efficient approach that meets both requirements is available to date.

With the efforts to develop tough hydrogels, our group has recently reported the facile preparation of hydrogen-bonded supramolecular polyvinyl alcohol (PVA)-glycerol gels that exhibit excellent thermoplastic and mechanical properties.[30] In this work, we employed PVA–glycerol gels as robust antifouling coating materials, and proposed the adhesion of these gels on substrates by using poly(allylamine hydrochloride) (PAH) hydrogel and ethyl α-cyanoacrylate (ECA) adhesives. Furthermore, the antifouling performance of PVA–glycerol hydrogels against barnacles was observed. Therefore, it is expected that our study would facilitate the practical application of hydrogels in marine antifouling.

2 Experimental section

2.1 Materials

Poly(vinyl alcohol) (PVA) (polymerization degree 1750 ± 50, 98%) was purchased from Sinopharm Chemical Reagent Co., Ltd (Shanghai, China), glycerol (AR) was purchased from Beijing Chemical Works (Beijing, China); poly(allylamine hydrochloride) (PAH) (M_n = 120 000–200 000), paraffin (AR) and 2,2,4-trimethylpentane (AR) were purchased from Beijing Innochem (Beijing, China); ethyl α-cyanoacrylate (ECA) was purchased from Guangdong Epida Adhesive Co., Ltd (Guangdong, China); pyrophosphoric acid (sodium salt, PPi) was purchased from Aladdin (Beijing, China).

2.2 Preparation of PVA–glycerol hydrogel coating[30]

16 g PVA was dissolved in 144 g mixed solvents of deionized water and glycerol in 1 : 1 mass ratio. The mixture was mechanically stirred for 2 h at 150 °C to ensure the dissolution of PVA. A reflux device was added to prevent water evaporation in the whole process. The PVA solution was transferred into the flat molds and cup molds. The solution in the flat modes was frozen at −15 °C for 24 h and then thawed at 25 °C for 24 h. The freeze–thaw process was cycled three times. Fig. S1 (ESI†) shows the cup and flat coatings.

2.3 Preparation of the PAH hydrogel[31]

0.4 wt% PAH solution and 4.0 wt% sodium pyrophosphate(PPi) solution were prepared. 13.2 mL PPi solution was slowly added to 250 mL PAH solution while the PAH solution was stirred at 300 rpm using cylindrical magnetic stir bars. The mixture was then left to rest to coagulate for 3 days or for a longer period of time. The illustration of the molecular structure of PAH is shown below.

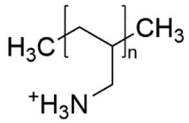

2.4 Preparation of ECA adhesive

A measured amount of ECA was thoroughly mixed with liquid paraffin or 2,2 4-trimethylpentane with different volume ratios (unless otherwise specified, paraffin was used, in $V_{ECA} : V_{paraffin}$ = 1 : 1). The illustration of the molecular structure of ECA is shown below.

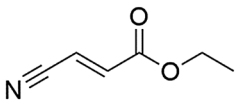

2.5 Mechanical test

The frozen–thawed gel samples were taken for preparation of test samples: some gel samples were used directly without any treatment; some were treated with pure ECA or diluted ECA adhesive on one side.

The tensile mechanical properties were measured using an Instron 3366 electronic universal testing machine (Instron Corporation, MA, USA) equipped with a 100 N load cell at a cross-head speed of 100 mm min^{-1}. The hydrogel samples were cut by DIN-53504 S3 mold (overall length: 35 mm; width: 6 mm; inner width: 2 mm; gauge length: 10 mm; thickness: 2 mm). At least 5 specimens were tested for each sample to obtain the average value.

The tensile stress σ_t was calculated by σ_t = load/(t·w) (t and w are the initial thickness and width of the dumbbell-shaped gel sample, respectively). The tensile strain ε_t is defined as the change in the length relative to the gauge length of the free standing specimen, and the tensile strength σ_b and the fracture tensile strain ε_b are, respectively, the tensile stress and the tensile strain at which the sample breaks. Stress and strain between ε_t = 10 ∼ 30% were used to calculate the initial elastic modulus (E).

2.6 Adhesion test

Two methods were used to carry out the adhesion test. (1) A half length of the gel strip (60 mm × 5 mm) was adhered to the stainless steel substrate with PAH hydrogel or ECA adhesive, respectively. The other end of the gel was clamped and was stretched at a speed of 40 mm min^{-1} until the gel was completely peeled off or broken. (2) A half length of the gel strip (60 mm × 5 mm) was adhered to the stainless steel substrate with ECA adhesive, and then a piece of PET film (60 mm × 5 mm × 0.1 mm), as a backing layer to prevent bulk deformation, was adhered to the outside surface of the gel with ECA adhesive. The other end of the gel was clamped and was stretched at a speed of 25 mm min^{-1} until the gel was completely peeled off or broken.

Peeling energy (G) refers to the energy consumed to completely peel the gel per unit area from the substrate; it can be

calculated as: $G = E/S = (F \cdot l)/(l \cdot d) = F/d$, *i.e.*, $G = F/d$. l and d are the length and width of the gel sample, respectively, S is the area of the adhesive part of the gel, F is the force used for peeling, E is the energy required to completely peel the gel and d is 5 mm. At least 5 specimens were tested for each sample to obtain the average value.

2.7 Stability test

The PVA–glycerol hydrogel samples were directly immersed in deionized water and weighed every 24 h, and simultaneously the shape changes of the samples were recorded. In addition, the PVA–glycerol hydrogel was adhered to the stainless steel substrate with PAH hydrogel or ECA adhesive, respectively, and the composite structure was placed in a 55 °C oven for water losing tests. The sample was weighed every 10 min, and then photographed after 50 min. After the water losing test, the sample was immersed in deionized water to absorb water and weighed after 24 h and 48 h, and photos were taken and recorded after the water absorbing process. The above-mentioned "water losing–water absorbing" process was repeated 5 times for each of the samples (*i.e.*, 5 cycles were performed). Furthermore, the above-mentioned "water losing–water absorbing" cycle experiments were carried out in simulated seawater with a salinity of 3.34%. The simulated seawater was prepared by dissolving sodium chloride (16.7 g), magnesium sulfate (11.1 g) and potassium chloride (5.6 g) in 1 L deionized water.

2.8 SEM characterization

The morphologies of the PVA–glycerol hydrogel before and after the stability test were observed using a field emission scanning electron microscope (FE-SEM, Hitachi S-4800, Japan), at an accelerating voltage of 3 kV. In order to prepare the samples for SEM, PVA–glycerol hydrogels were cut into slices and frozen using liquid nitrogen for 10 min, then transferred into a vacuum freeze drier (Biocool FD2-1B-50, China) immediately and dehydrated for 24 h. Prior to observation, the samples were sputter-coated with gold to enhance the conductivity.

2.9 Bioassay for antifouling potency of PVA–glycerol hydrogel against the barnacle *Balanus albicostatus*

Adults of the barnacle *B. albicostatus* were collected from the intertidal zone in Xiamen, China. In the laboratory, the barnacle nauplii were released from the adults and reared to cyprids following the method of Feng *et al.*[32] The cyprids were used in the bioassay here, considering that barnacle settlement takes place in the cyprid stage.

PVA–glycerol hydrogel samples were prepared in specified shape and size, numbered 1# and 2#. Sample 1# is a PVA–glycerol hydrogel sample that has not been soaked in deionized water before being used for the bioassay, and sample 2# is the one that is fully soaked in deionized water. The purpose of soaking in deionized water here is to minimize the effects of glycerol. The experiment was performed with 6-well polystyrene plates (Innochem). The 1# and 2# PVA–glycerol hydrogel samples were placed close to the surfaces of the wells to cover the wall and bottom of the wells. Filtered (0.22 μm) seawater (5 mL, FSW) and about 20 cyprids were added to each well with PVA–glycerol hydrogel. At the same time, to test the effect of glycerol on the settlement and survival of the barnacle cyprids, glycerol was dissolved in FSW, with test concentrations of 1%, 3%, 5%, 8%, and 10% (v/v). A volume of 5 mL of each glycerol solution and about 20 cyprids were added to each well. FSW in the wells without PVA–glycerol hydrogel was used as the control. Three replicates were set up for each treatment. The 6-well plates were incubated in the dark at 25 °C for 48 h, after which the number of cyprids that had settled, died or were still swimming was counted under a stereomicroscope. Statistical analysis was carried out using SPSS version 22.0. Differences in barnacle settlement or mortality between treatments were analyzed by one-way ANOVA followed by a Tukey *post hoc* test. The significance level was set at $P < 0.05$.

To check whether PVA–glycerol hydrogel maintains its antifouling potency after the water losing–water absorbing process, we prepared a third PVA–glycerol hydrogel sample (3#) and tested it against *B. albicostatus* cyprids following the procedures described above. The preparation process of these 3# PVA–glycerol hydrogel samples is as follows. Firstly, the cup shaped hydrogel, whose size and shape match the round hole of the 6-well polystyrene plate, was adhered to the 6-well polystyrene plate by ECA solution ($V_{ECA} : V_{paraffin} = 1 : 1$). The whole 6-well polystyrene plate/gel composite structure was then subjected to five cycles of the "water losing–water absorbing" process (the water losing procedure was carried out at 55 °C for 50 min, and the water absorbing time was 48 h (room temperature)). The composite structure was immersed in deionized water for 24 h before the biological experiment. For the bioassay, the wells containing only FSW and cyprids were used as the control. Difference in barnacle settlement or mortality between the 3# sample and the control was analyzed using a Student's *t*-test.

3 Results and discussion

3.1 Adhesion ability

The bonding fastness between the hydrogel coating and the substrate determines the life of the coating. In this work, we used stainless steel as substrates for research. When the hydrogel was directly coated on the stainless steel plate surface, it was found that the hydrogel adhesion was not strong, and the entire coating could be peeled off with tweezers easily. In order to improve the adhesion of the hydrogel to the surface of the substrate, two substances PAH hydrogel and ECA were employed as binders, and their contribution to the adhesion between the PVA–glycerol hydrogel and the substrate was examined, respectively.

Typically, PAH hydrogel is formed by ionic cross-linking of PAH polyelectrolytes and PPi ion *via* electrostatic interactions in aqueous solution, and consequently it is also called "ionic gel". There is a strong interaction between the ionic hydrogel and the metal, so that it can be firmly adhered to the surface of the metal material.[31] Since PAH hydrogel is a soft matter with strong polarity, it was expected that it has strong adhesion to PVA–glycerol gel, which is also a soft matter constructed by

polar polymer molecules. Thus, the PAH hydrogel was selected as an adhesive to stick the PVA hydrogels onto metal surfaces.

Ethyl α-cyanoacrylate (ECA) is a kind of single-component fast-setting adhesive that cures very quickly at room temperature. Wirthl *et al.*[33] have done a lot of studies on bonding hydrogels to diverse materials using ECA as a binder. During contact with the hydrogel or the metal substrate, the ECA monomer can undergo rapid polymerization under the action of water molecules in the air and the hydrogel to form polymer chains that show good adhesion to both metals and hydrogels, thereby tightly bonding the two together. Based on the polar interaction between the adhesive and the objects, hard materials are adhered using adhesives with polar polymers as the main solid components since antiquity. So, the adhesion mechanism between ECA and metal is not difficult to understand. However, the adhesion mechanism between ECA and the hydrogel is confusing. In a recent paper,[34] extensive studies have been performed on the use of cyanoacrylate for soft material bonding, and the concept of "molecular staples" was proposed. The authors assumed that when two hydrogels are glued with diluted cyanoacrylate, the cyanoacrylate molecules diffuse into the hydrogel, the two hydrogels are then adhered by the islands of polycyanoacrylate formed *in situ* at their interface. The polycyanoacrylate molecules of the islands are in topological entanglement with the polymer networks of the hydrogels. This helps us understand the puzzling questions above.

The contributions of these two adhesives to the adhesion between the PVA–glycerol hydrogel and the substrate were examined by the peeling experiment as shown in Fig. 1, respectively. The force/width-displacement curves of the PVA glycerol hydrogel/stainless steel substrate composite structure in Fig. 1a indicate the use of PAH hydrogel obtained at different standing times. When using a PAH hydrogel prepared under the condition of standing for 3 days, the composite structure had a peeling energy of 317 J m^{-2}, while the peeling energy increased to 460 J m^{-2} when it was for one month. It can be seen that the presence of PAH hydrogel enhances the bonding between the PVA–glycerol gel coating and the substrate greatly, and the adhesion ability of the PAH hydrogel is more exceptional when the solution system is allowed to stand for a longer period of time during the preparation process.

For the case of using ECA as a binder, ECA needs to be formulated into a solution system with a diluent in a certain ratio. This is because the polymerization of pure ECA initiated by the water in the hydrogel is too quick for the adhesive to penetrate into the hydrogels, thus leading to insufficient adhesion between the hydrogel and the substrate. After mixing with an alkane solvent, the polymerization rate of the diluted cyanoacrylate is greatly delayed, as a result, the time is sufficiently long to let the monomer penetrate into the hydrogel. Our studies have shown that as the proportion of diluent in the ECA binder system increases, the time required for firm adhesion of the PVA–glycerol hydrogel to the substrate increases. When the ratio of ECA to diluent is less than 1 : 2 (volume ratio), there is substantially no obvious stickiness to the PVA–glycerol/stainless steel substrate combination. That is to say, the proportion of diluent in the ECA binder system should be neither too low nor too high. Systems with a ratio of ECA to diluent (paraffin) of 2 : 1 and 1 : 1 (volume ratio) were used for PVA–glycerol

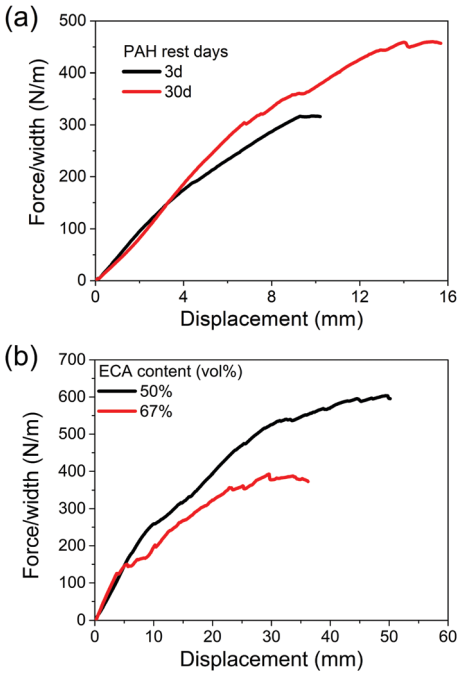

Fig. 1 Results of the peeling tests of PVA–glycerol hydrogels bonded to stainless steel plates using PAH gels (a) and ECA's paraffin solution (b) as the binder, respectively. Adhesion test conditions: without PET film as a backing layer on the surface of the gel, and the stretching speed was 40 mm min^{-1}.

gel/stainless steel substrate bonding. When the bonded composite structure was subjected to peeling measurement, it was found that the PVA–glycerol gel was first broken before peeling occurred, indicating that the bonding strength was higher than the tensile strength of the gel itself. Although the peeling energy of the sample could not be measured, a minimum peeling energy value was able to be calculated according to the maximum force before breaking. Fig. 1b shows the force/width–displacement curves of the composite structure with the ECA solution as the binder. The peeling energy before fracture was calculated to be more than 603 J m^{-2} when an ECA to paraffin ratio of 1 : 1 was used. However, an increase of the ECA content in the binder caused a decrease in the strength of the PVA–glycerol gel itself. The PVA–glycerol gel with an ECA to paraffin ratio of 1 : 1 broke at a load of 3.01 N. In contrast, the breaking load reduced to 1.96 N for the 2 : 1 system of ECA solution (the sizes of the tested samples are the same).

3.2 Stability

The target product of this study is the anti-marine biological pollution material working in the water environment. Therefore, we examined the stability of the PVA–glycerol hydrogel coating itself and the hydrogel/stainless steel structure in water, respectively.

3.2.1 Composition stability of the hydrogel. The composition change of the PVA–glycerol hydrogel after immersion in deionized water was investigated first. Fig. 2 shows the mass change of a PVA–glycerol hydrogel with time in deionized water. It can be seen

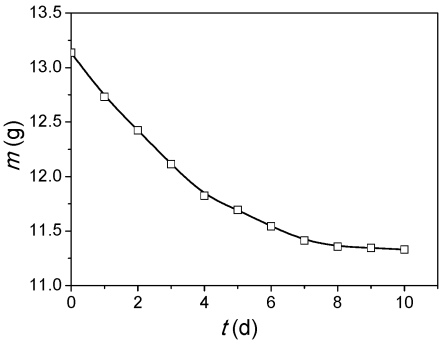

Fig. 2 Mass change of PVA–glycerol hydrogel in deionized water.

from Fig. 2 that the mass of the gel declines more obviously at the beginning of the period; as the immersion time is prolonged, the decline rate in mass gradually decreases and the final mass remains substantially constant. For the PVA–glycerol hydrogels in this work, the PVA molecular chains realize physical cross-linking by forming an intermolecular hydrogen bond with the glycerol molecule,[30] and a three-dimensional network structure is built. The glycerol molecules that are not involved in the formation of the network structure in the system, called free glycerol molecules, are easily released from the interior of the gel into the water when the system is in contact with water, resulting in the mass loss of the PVA–glycerol hydrogels. When the free glycerol component is completely released, the mass of the hydrogel no longer changes.

During the whole life cycle of a ship, it is not always in water, and there will be times when it leaves the water. Therefore, in practical applications, the hydrogel coating on the surface of the hull will undergo multiple "water losing–water absorbing" processes. Herein, we performed a "water losing–absorbing" cycle experiment with a PVA–glycerol hydrogel/stainless steel substrate in deionized water and simulated seawater. The changes in the gel mass are examined, and the results are shown in Fig. S2 (ESI†). Fig. S2a and c (ESI†) show the mass changes of the PVA–glycerol hydrogel with drying times of each cycle when the composite structure undergoes "water absorbing" in deionized water and simulated seawater, respectively. It can be seen that whether in deionized water or simulated seawater, the mass of the PVA–glycerol hydrogel decreases linearly during the drying process of each cycle, and the water loss rate remains stable, which indicates that there was no significant change in the pore size of the gel itself during the "water losing–absorbing" cycle. In other words, the network structure of the gel did not change significantly.

Fig. S2b and d (ESI†) show the sample mass of several typical samples after 48 h of water absorption in each "water losing–absorbing" cycle. In experiments with deionized water systems, PVA–glycerol hydrogels experienced partial mass loss after each cycle (Fig. S2b, ESI†). The total mass loss percentage after 5 cycles was comparable to the final mass loss percentage when the free hydrogel was immersed in deionized water for 10 days. For the simulation of the seawater system, as shown in Fig. S2d (ESI†), the PVA–glycerol hydrogel showed a significant mass loss during the first two cycles, and the last three cycles had only minor mass changes. The difference in mass losing rates in deionized water and simulated seawater can be attributed to the fact that the osmotic pressure of the simulated seawater is higher than the osmotic pressure of the deionized water, so that the free glycerol molecules diffuse to the external water environment more quickly, whereas, the final total mass loss percentage in seawater is close to the mass loss percentage while resting in deionized water (Table 1). This indicates that the mass loss of the gel after multiple cycles is mainly due to the loss of free glycerol molecules of the system. Furthermore, we can infer that the network structure of the gel had not changed significantly upon multiple water losing–water absorbing process cycles, as the PVA–glycerol hydrogel no longer exhibited obvious mass changes during the last three cycles. The SEM

Table 1 Mass change of PVA–glycerol hydrogel samples

Sample	Percentage of mass loss (%)
PVA–glycerol hydrogel[a]	13.8
PVA–glycerol hydrogel with adhesive[b]	11.7
PVA–glycerol hydrogel with adhesive[c]	12.4

[a] The free PVA–glycerol hydrogel, the corresponding data were calculated after immersion in deionized water for 10 d. [b] PVA–glycerol hydrogels adhered to the stainless steel cup by ECA adhesive in deionized water, the corresponding data were calculated after 5 cycles of "water losing–water absorbing" processes. [c] PVA–glycerol hydrogels adhered to the stainless steel cup by ECA adhesive in simulated seawater, the corresponding data were calculated after 5 cycles of "water losing–water absorbing" processes.

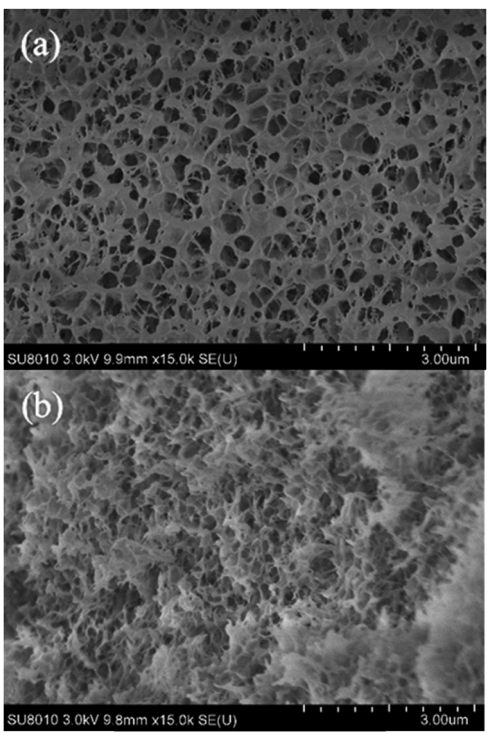

Fig. 3 SEM images of PVA–glycerol gels. (a) The as-prepared PVA–glycerol gel. (b) The PVA–glycerol gel after 5 cycles of "water losing–absorbing" processes in deionized water.

results shown in Fig. 3 further confirm the above inference. The morphology of the PVA–glycerol gel after 5 cycles of "water losing–absorbing" processes was similar to the as-prepared one, and no obvious collapse or deformation of the porous structure was observed.

3.2.2 Adhesion stability of the gel coating. In an ideal situation, if the hydrogel forms a complete coating on the surface of the hull, and the water does not intrude into the interface between the gel and the metal, the adhesion stability of the gel coating on the metal substrate should be maintained. However, if local debonding of the hydrogel coating occurs during the "water losing–absorbing" process, water can easily invade the interface between the two, which may affect the combination. Therefore, we prepared a planar gel/stainless steel plate system, and a curved gel/stainless steel cup system and subjected them to a "water losing–absorbing" process to investigate if the hydrogel adhered stably to the substrate.

Fig. 4 shows photographs reflecting the stability of the gel coating adhesion of a "planar gel/stainless steel plate" system. Among them, Fig. 4a and b are samples using PAH hydrogel as a binder. It can be seen from the appearance that the PAH hydrogel could maintain good viscosity after the first "water losing–absorbing" process, but after the second "water losing–absorbing" cycle, the PAH hydrogel became hard and brittle and no longer had the ability to adhere to the PVA–glycerol hydrogel coating. Fig. 4c and d show the situation when using ECA adhesive. After two cycles of the "water losing–absorbing" process, the PVA–glycerol hydrogel remained firmly adhered to the stainless steel plate, indicating that the ECA adhesive has excellent resistance to water intrusion.

Fig. 5 shows photographs of the "gel/stainless steel cup" composite structure after different "water losing–absorbing" cycles in deionized water. Since PAH hydrogels perform poorly in "planar gel/stainless steel plate" systems, we only used ECA adhesives to adhere PVA–glycerol hydrogels to stainless steel cups to make composite structures. The results showed that the PVA–glycerol hydrogel coating became thinner after losing water, but did not lose the soft feature of hydrogels (Fig. 5a). The overall shape of the gel layer remained intact and there was no deformation or shedding due to heat shrinkage. Fig. 5b shows the photographs just after each water absorption. The PVA–glycerol hydrogel recovered its initial shape and morphology, also no deformation or shedding occurred. Compared to the initial state, the morphology of the gel layer on the composite structure did not change significantly after the fifth "water losing–absorbing" process, indicating that the stability of the composite structure is good. We also investigated the adhesion stability of the "gel/stainless steel cup" composite structure in simulated seawater, and the result indicated a unanimous conclusion as shown in Fig. S3 (ESI†).

Fig. 6 shows the peeling energy (G) of the "planar gel/stainless steel plate" systems undergoing 1–5 "water losing–absorbing" cycles, respectively. Compared with the original sample, the peeling energy of the composite structure after the first "water losing–absorbing" cycle decreased by 13.7%, and the values of G mainly remain constant after the second and third "water losing–absorbing" cycles. But for the samples after the fourth and fifth "water losing–absorbing" cycles, the G value drops to about 74% of the original value. The above results indicate that multiple "water losing–water absorbing" processes have some influence on the binding strength of the composite structure.

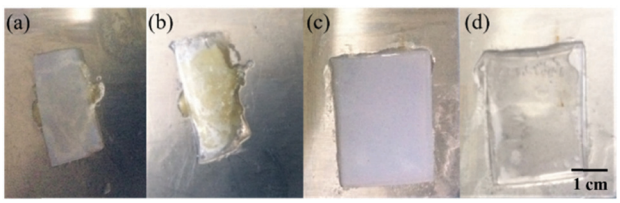

Fig. 4 Photographs of the "planar gel/stainless steel plate" composite structure. (a and b) PVA–glycerol hydrogel adhered to the stainless steel plate by PAH enduring the "water losing–absorbing" process of the first cycle (a) and the second cycle (b); (c and d) PVA–glycerol hydrogel adhered to the stainless steel plate by ECA adhesive (2,2,4-trimethylpentane solution of ECA, with a concentration of 50 vol%) enduring the "water losing–absorbing" process of the first cycle (c) and the second cycle (d).

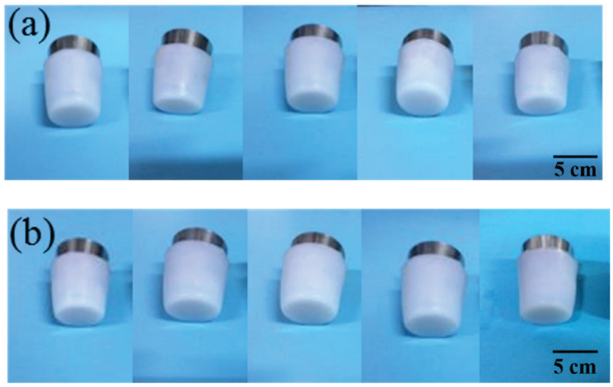

Fig. 5 Photographs of the "PVA–glycerol gel/stainless steel cup" composite structure with ECA adhesive after several "water losing–absorbing" cycles in deionized water. Photos from left to right refer to samples after 1, 2, 3, 4 and 5 cycles of water losing (a) and absorbing processes (b), respectively.

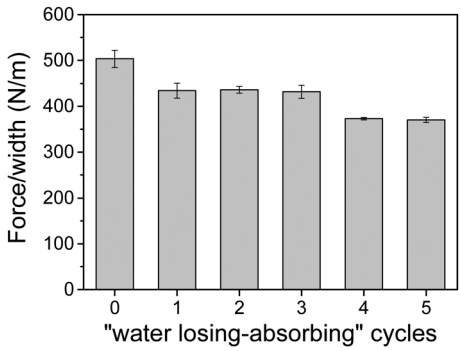

Fig. 6 The effects of "water losing–absorbing" cycles on peeling energy of "planar gel/stainless steel plate" systems using ECA solution (V_{ECA} : $V_{paraffin}$ = 1 : 1) as the binder. Sample preparation: the water losing procedure was carried out at 55 °C for 50 min, and the water absorbing time was 48 h (room temperature); adhesion test conditions: with PET film as a backing layer on the outside surface of the gel, and the stretching speed was 25 mm min^{-1}.

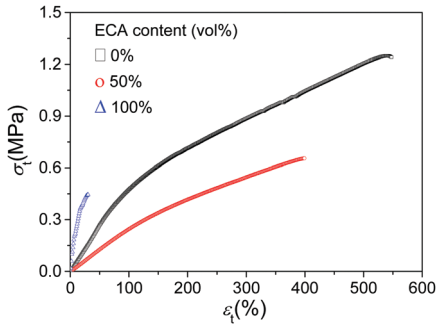

Fig. 7 Typical σ_t–ε_t curves of the PVA–glycerol gels treated with a paraffin solution of ECA.

3.3 Tensile mechanical properties

The mechanical properties of the PVA–glycerol hydrogel itself treated with different ECA solutions were investigated by the tensile tests. As shown in Fig. 7, the gel sample which was not treated with an ECA binder had a tensile strength (σ_b) of 1.23 ± 0.07 MPa, an elongation at break (ε_b) of 544 ± 32%, and a modulus (E) of 0.51 ± 0.03 MPa. The tensile strength value was higher compared with those of Shi's PVA–glycerol gels[30] because of the increased freeze–thaw times. For the gel sample treated with a 1 : 1 diluted ECA binder, the σ_b was 0.64 ± 0.16 MPa, ε_b was 385 ± 127% and E was 0.28 ± 0.02 MPa. The standard error in this group was high since it was difficult to spread the adhesive evenly. For the gel sample treated with an undiluted ECA binder, the σ_b was 0.41 ± 0.08 MPa, ε_b was 19 ± 7% and E was 1.74 ± 0.02 MPa. The above results indicate that the ECA binder causes a significant decrease in the strength of the PVA–glycerol gel, and the higher the ECA content in the used ECA solution, the worse the elasticity of the PVA–glycerol gel becomes, which is consistent with the observation from the adhesion ability tests.

3.4 Effects of the hydrogel and the glycerol on the settlement and survival of barnacle cyprids

Here the antifouling potency of the hydrogel against barnacles was tested. Since hydrogels contain free glycerol (sample 1#), we also tested hydrogel samples that had been soaked in deionized water to remove free glycerol (sample 2#). Furthermore, we examined the effect of pure glycerol on the settlement and survival of barnacle cyprids. The results are shown in Table 2.

It can be seen from Table 2 that the settlement percentage in treatments with 1–10% glycerol solution was significantly lower than that in the control, indicating that glycerol is active in inhibiting barnacle settlement. This inhibitive activity was concentration-dependent, as the settlement percentage decreased with the increase of the concentration of glycerol. The unsettled cyprid larvae were mostly or all dead in the glycerol treatments. For example, in the treatment with 1% glycerol solution, the non-settlement percentage (non-settlement percentage = 100% − settlement percentage) was 30.9%, which was the same as the mortality (30.9%). This suggests that the inhibition of glycerol against larvae settlement is mainly caused by its toxicity. In the test with PVA–glycerol hydrogel, none of the cyprids were settled and all of them were dead in the treatment with 1# gel sample,

Table 2 Effects of hydrogels and glycerol on the settlement and survival of barnacle cyprids

Treatment	Settlement percentage (mean ± SE, %)	Mortality (mean ± SE, %)
Control	94.8 ± 2.6^{a}	1.3 ± 1.3^{a}
1# hydrogel sample	0.0 ± 0.0^{b}	100.0 ± 0.0^{b}
2# hydrogel sample	0.0 ± 0.0^{b}	36.5 ± 5.4^{c,d}
1% glycerol solution	69.1 ± 8.7^{a}	30.9 ± 8.7^{c}
3% glycerol solution	36.8 ± 11.1^{c}	60.8 ± 9.6^{d,e}
5% glycerol solution	32.4 ± 5.3^{c}	65.9 ± 4.5^{e}
8% glycerol solution	0.0 ± 0.0^{b}	100.0 ± 0.0^{b}
10% glycerol solution	0.0 ± 0.0^{b}	100.0 ± 0.0 ^{b}

Note: different lowercase letters after the values in the same column indicate significant differences among treatments ($P < 0.05$).

Table 3 Effects of the PVA–glycerol gel after 5 cycles of the "water losing–water absorbing" process

Treatment	Settlement percentage (mean ± SE, %)	Mortality (mean ± SE, %)
Control	97.6 ± 1.3^{a}	1.4 ± 1.4^{a}
3# hydrogel sample	0.0 ± 0.0^{b}	30.7 ± 3.7^{b}

Note: different lowercase letters after values in the same column indicate significant differences among treatments ($P < 0.05$).

indicating that the 1# gel sample has a strong toxic effect on barnacle cyprids, which may be due to the release of free glycerol from the hydrogel. Therefore, the result of 1# sample could not confirm whether or not the gel itself has antifouling potency. In the treatment with 2# gel sample, all cyprids were unsettled, but only 36.5% cyprids were dead, which suggests that compared to the 1# sample, the toxicity of the hydrogel sample was greatly reduced after immersion in deionized water. Furthermore, larval mortality in the 2# gel sample was close to that in the 1% glycerol solution, indicating that these two treatments had similar toxicity, but the settlement percentage was remarkably different (0% in the 2# sample and 69.1% in the 1% glycerol solution). In the 1% glycerol solution, all the alive barnacle cyprids (69.1%) were settled, while in the 2# sample, about 63.5% of the barnacle cyprids were alive but none of them settled on the surface of the gel, which indicates that the 2# sample has a strong inhibition effect on barnacle settlement, and the inhibition effect is mainly caused by the hydrogel sample itself.

Furthermore, after five cycles of the water losing–water absorbing process, the hydrogel maintained its inhibition effect on barnacle settlement (Table 3). In the 3# sample, 69.3% of the cyprids were alive but none of the cyprids settled, while in the control, most cyprids (97.6%) showed settlement, suggesting the high antifouling potency of the 3# sample. It is noteworthy that the antifouling potency of the 3# sample (Table 3) appears to be similar to that of the 2# sample (Table 2).

4 Conclusions

In this paper, we used PVA–glycerol hydrogels as the coating material, and selected PAH hydrogel and ECA as binders to

adhere the PVA–glycerol gel coating onto the metal (stainless steel) substrate, and investigated the stability of this composite structure under a variety of environmental conditions. Also, the antifouling effect of PVA–glycerol hydrogels was tested against the barnacle *Balanus albicostatus.* It has been found that PVA–glycerol hydrogels can be firmly adhered to a stainless steel substrate by using PAH hydrogels or ECA as binders. For the ECA adhesive, the proportion of diluent in the ECA solution affects its adhesion greatly. With appropriate formulation, the adhesion of ECA is better than that of the PAH hydrogel. The composite structure with PAH hydrogel as the binder can maintain stability in the underwater environment, but it can be easily damaged when in a dehydrating environment. In contrast, the excellent adhesive ability of the ECA binder can be retained after several water losing–water absorbing cycles, although the presence of ECA binder may have a certain undesirable effect on the strength of the PVA–glycerol hydrogel. The PVA–glycerol hydrogel itself can maintain its shape stability during the repeated "water losing–water absorbing" processes. The settlement bioassays with barnacle cyprids showed that the PVA–glycerol hydrogel has a strong settlement-inhibiting effect on the barnacle cyprids, and this inhibition effect is mainly caused by the hydrogel itself rather than the release of the glycerol from the hydrogel. Furthermore, the PVA–glycerol hydrogel maintains its antifouling potency after repeated cycles of the "water losing–water absorbing" process. Therefore, the use of the PVA–glycerol hydrogel as a protective coating for the hull and ECA as adhesive may help to solve the problem of marine biofouling.

Conflicts of interest

The authors declare no competing financial interests.

Acknowledgements

We appreciate financial support from the Project of Subsidy Funds for Marine Economic Development in Fujian Province under Grant FJHJF-L-2018-2, and the Open Fund of State-Province Joint Engineering Laboratory of Marine Bioproducts and Technology in Xiamen University under Grant 201806.

References

1 J. A. Callow and M. E. Callow, *Nat. Commun.*, 2011, **2**, 244.
2 M. P. Schultz, J. A. Bendick, E. R. Holm and W. M. Hertel, *Biofouling*, 2011, **27**, 87–98.
3 M. P. Schultz, *Biofouling*, 2007, **23**, 331–341.
4 I. B. Beech and J. Sunner, *Curr. Opin. Biotechnol.*, 2004, **15**, 181–186.
5 I. B. Beech, J. A. Sunner and K. Hiraoka, *Int. Microbiol.*, 2005, **8**, 157–168.
6 I. K. Konstantinou and T. A. Albanis, *Environ. Int.*, 2004, **30**, 235–248.
7 S. Kiil, C. E. Weinell, M. S. Pedersen and K. Dam-Johansen, *Ind. Eng. Chem. Res.*, 2001, **40**, 3906–3920.
8 Y. Yonehara, H. Yamashita, C. Kawamura and K. Itoh, *Prog. Org. Coat.*, 2001, **42**, 150–158.
9 U. Goransson, M. Sjogren, E. Svangard, P. Claeson and L. Bohlin, *J. Nat. Prod.*, 2004, **67**, 1287–1290.
10 C. Hellio, M. Tsoukatou, J.-P. Maréchal, N. Aldred, C. Beaupoil, A. S. Clare, C. Vagias and V. Roussis, *Mar. Biotechnol.*, 2005, **7**, 297–305.
11 M. Lejars, A. Margaillan and C. Bressy, *Chem. Rev.*, 2012, **112**, 4347–4390.
12 J. P. Brady, G. A. Ayoko, W. N. Martens and A. Goonetilleke, *Mar. Pollut. Bull.*, 2014, **89**, 464–472.
13 A. A. Keller, A. S. Adeleye, J. R. Conway, K. L. Garner, L. Zhao, G. N. Cherr, J. Hong, J. L. Gardea-Torresdey, H. A. Godwin, S. Hanna, Z. Ji, C. Kaweeteerawat, S. Lin, H. S. Lenihan, R. J. Miller, A. E. Nel, J. R. Peralta-Videa, S. L. Walker, A. A. Taylor, C. Torres-Duarte, J. I. Zink and N. Zuverza-Mena, *NanoImpact*, 2017, **7**, 28–40.
14 A. S. Adeleye, E. A. Oranu, M. Tao and A. A. Keller, *Water Res.*, 2016, **102**, 374–382.
15 D. Carteau, K. Vallee-Rehel, I. Linossier, F. Quiniou, R. Davy, C. Compere, M. Delbury and F. Fay, *Prog. Org. Coat.*, 2014, **77**, 485–493.
16 P. J. Earley, B. L. Swope, K. Barbeau, R. Bundy, J. A. McDonald and I. Rivera-Duarte, *Biofouling*, 2014, **30**, 51–68.
17 K. Mochida, K. Ito, M. Ito, T. Hano and N. Ohkubo, *Comp. Biochem. Physiol., Part C: Toxicol. Pharmacol.*, 2018, **214**, 61–67.
18 M. S. Selim, M. A. Shenashen, S. A. El-Safty, S. A. Higazy, M. M. Selim, H. Isago and A. Elmarakbi, *Prog. Mater. Sci.*, 2017, **87**, 1–32.
19 W. J. Yang, K. G. Neoh, E. T. Kang, S. L. M. Teo and D. Rittschof, *Prog. Polym. Sci.*, 2014, **39**, 1017–1042.
20 S. Kim, T. Gim and S. M. Kang, *ACS Appl. Mater. Interfaces*, 2015, **7**, 6412–6416.
21 W. Yandi, S. Mieszkin, P. Martin-Tanchereau, M. E. Callow, J. A. Callow, L. Tyson, B. Liedberg and T. Ederth, *ACS Appl. Mater. Interfaces*, 2014, **6**, 11448–11458.
22 T. P. Galhenage, D. C. Webster, A. M. S. Moreira, R. J. Burgett, S. J. Stafslien, L. Vanderwal, J. A. Finlay, S. C. Franco and A. S. Clare, *J. Coat. Technol. Res.*, 2016, **14**, 307–322.
23 M. J. Vucko, A. J. Poole, C. Carl, B. A. Sexton, F. L. Glenn, S. Whalan and R. de Nys, *Biofouling*, 2014, **30**, 1–16.
24 M. S. Selim, S. A. El-Safty, M. A. El-Sockary, A. I. Hashem, O. M. A. Elenien, A. M. El-Saeed and N. A. Fatthallah, *RSC Adv.*, 2015, **5**, 63175–63185.
25 C. Liu, C. F. Ma, Q. Y. Xie and G. Z. Zhang, *J. Mater. Chem. A*, 2017, **5**, 15855–15861.
26 T. Murosaki, T. Noguchi, A. Kakugo, A. Putra, T. Kurokawa, H. Furukawa, Y. Osada, J. P. Gong, Y. Nogata, K. Matsumura, E. Yoshimura and N. Fusetani, *Biofouling*, 2009, **25**, 313–320.
27 T. Murosaki, T. Noguchi, K. Hashimoto, A. Kakugo, T. Kurokawa, J. Saito, Y. M. Chen, H. Furukawa and J. P. Gong, *Biofouling*, 2009, **25**, 657–666.
28 L. Y. Xie, F. Hong, C. X. He, C. F. Ma, J. H. Liu, G. Z. Zhang and C. Wu, *Polymer*, 2011, **52**, 3738–3744.
29 F. Hong, L. Y. Xie, C. X. He, J. H. Liu, G. Z. Zhang and C. Wu, *Polymer*, 2013, **54**, 2966–2972.

30 S. J. Shi, X. Peng, T. Q. Liu, Y. N. Chen, C. C. He and H. L. Wang, *Polymer*, 2017, **111**, 168–176.
31 Y. Huang, P. G. Lawrence and Y. Lapitsky, *Langmuir*, 2014, **30**, 7771–7777.
32 D. Feng, C. Ke, S. Li, C. Lu and F. Guo, *Mar. Biotechnol.*, 2009, **11**, 153–160.
33 D. Wirthl, R. Pichler, M. Drack, G. Kettlguber, R. Moser, R. Gerstmayr, F. Hartmann, E. Bradt, R. Kaltseis, C. M. Siket, S. E. Schausberger, S. Hild, S. Bauer and M. Kaltenbrunner, *Sci. Adv.*, 2017, **3**, e1700053.
34 B. Chen, J. Yang, R. Bai and Z. Suo, *Adv. Healthcare Mater.*, 2019, e1900810.